Solid-Phase Grafting of Hydroxymethyl Acrylamide onto Polypropylene through Pan Milling

CHANGSHENG LIU, QI WANG

The State Key Laboratory of Polymer Materials Engineering, Polymer Research Institute of Sichuan University, Chengdu 610065, People's Republic of China

Received 10 September 1999; accepted 22 March 2000

ABSTRACT: The solid-phase graft polymerization of hydroxymethyl acrylamide (HMA) onto polypropylene (PP) was realized by employing our self-designed pan-type milling equipment which has a unique and smart structure and can exert quite strong shear forces and pressure on the materials in between and break them down. When PP particles and HMA are pan-milled together, the macromolecular radicals generated from the chain scission of PP under stress can initiate HMA to polymerize, forming the PP-*g*-HMA graft copolymer. The graft copolymers were characterized by chemical titration, FTIR, DSC, and contact angle measurement. The amount of grafted HMA depends on the HMA concentration, increase of the PP particles' surface area during pan milling, temperature, as well as rotation speed of the mill pan. The percentage of grafting reaches 2.43%. The particle-size analysis showed that PP with a larger particle size favors the graft polymerization of HMA onto PP. DSC analysis demonstrated that the crystallinity of PP-*g*-HMA decreases as compared with PP due to the grafting of HMA onto PP. © 2000 John Wiley & Sons, Inc. J Appl Polym Sci 78: 2191–2197, 2000

Key words: mechanochemistry; functionalization; polypropylene; hydroxymethyl acrylamide; solid-phase grafting

INTRODUCTION

Polymer mechanochemistry is a frontier science based on mechanics and polymer chemistry. It studies polymer reactions induced by stress. The mechanochemical procedures of polymers may be divided into stress activation, stress degradation, and stress synthesis. When suffering from stress, polymer bonds are distorted and bond angles and distance are extended, and when the imposed stress is beyond the chemical bonding energy, bond rupture occurs. This produces macromolecular radicals, which may be terminated either by disproportionation or radical traps, resulting in the reduction of the molecular weight of the polymer (i.e., polymer degradation) or, by other radical reactions, giving block or graft copolymers and branched or crosslinked polymers (i.e., stress synthesis). Polymer mechanochemistry offers a new route for the preparation and modification of polymer materials and is important for both academic research and practical applications.[1–8]

In our previous articles,[9–11] a self-designed pan-type equipment for pulverizing and mixing and the stress reactions of solid polymers and fillers or monomers was reported. The key part of this equipment is the mill pan; its ingenious structure is drawn from the traditional Chinese stonemill. The main structure parameters of the mill pan are the radius R, division number in each division m, bevel angle α, and slot top width δ.[11] Theoretical analysis of the milling process[9]

Correspondence to: Q. Wang.

Contract grant sponsors: China Petro-Chemical Science &Technology Development Corp.; Polyamide Research Center of China Petro-Chemical General Corp.

Journal of Applied Polymer Science, Vol. 78, 2191–2197 (2000)

demonstrated that the milling process is similar to that of cutting material using scissors; more than this, the bevels of the mill pan squeeze and split the materials in between in a three-dimensional way. The equipment can exert quite a strong shear force and pressure on the materials in between and break them down.[9,12] When polypropylene (PP) particles and vinyl monomers are pan-milled together at room temperature, the macromolecular radicals generated from the chain scission of PP under stress can initiate a vinyl monomer to polymerize, forming a graft copolymer.

PP is one of the most important commodity plastics because of its low cost, high performance, and wide application. However, the poor compatibility of PP with polar polymers or fillers due to the nonpolar feature of PP limits its even wider application. Grafting polar monomers onto PP offers an effective way to enhance the polarity of PP. The graft polymerization of polar monomers onto PP is usually conducted with chemical initiators in solution, melt, or the solid state. The reaction temperature, even for solid-phase grafting, is over 100°C.[13–17]

In this article, we report the solid-phase grafting of hydroxymethyl acrylamide (HMA) onto PP by using the self-designed pan-type mill equipment. The effects of various factors such as the HMA/PP ratio, number of milling cycles, temperature, and rotation speed of the pan mill on the amount of grafted HMA in PP-*g*-HMA were investigated. The structure and properties of the graft copolymer PP-*g*-HMA were studied using FTIR, DSC, particles-size analysis, surface-area analysis, contact angle test, mechanical property test, etc.

EXPERIMENTAL

Materials

PP, T30s, with a pellet diameter of 3–4 mm was from the Dushanzi Petrochemical Co. (Kelamayi, China). HMA was from the Tianjing Chemical Plant (Tianjing, China).

Equipment

The self-designed pan-type mill equipment was used. Details of the equipment were reported in refs. 9 and 11.

Solid-phase Grafting of HMA onto PP

PP-*g*-HMA was prepared by comilling PP and HMA with the pan-type milling equipment at ambient temperature. The product was extracted with water three times for 72 h to remove the unreacted monomer, then dried under a vacuum at 60°C.

Characterization

The percentage of grafting was determined by chemical titration according to the method reported in ref. 18:

$$\% \text{ grafting} = \frac{C \times \Delta V \times M}{4 \times 1000 \times W} \times 100\% \qquad (1)$$

where C is the concentration of sodium thiosulfate aqueous solution; ΔV, the volume difference of the sodium thiosulfate aqueous solution used in titration of the blank sample and titration of the PP-*g*-HMA sample; M, the molecular weight of HMA; and W, the weight of the PP-*g*-HMA sample.

PP and the grafting copolymers were compression-molded into thin films on a compression-molding machine at 190°C under 100 kg/cm^2 pressure. IR spectra of these films were recorded with a Nicolet 20 SXB FTIR spectrometer.

Contact angle measurements were made with a Contact-θ-Meter developed at ERMA Optical Works Co., Ltd. (Japan). PP or PP-*g*-HMA films were compression-molded and water was used as a liquid.

Differential scanning calorimetric studies were conducted using a Perkin–Elmer DSC7 thermal analyzer. The analysis was carried out at a constant heating or cooling rate of 10°C/min in the temperature range of 25–200°C under a nitrogen atmosphere. The crystallinity of various samples was calculated according to the following expression:

$$\% \text{ Crystallinity} = (\Delta H_f^*/\Delta H_f^0) \times 100 \qquad (2)$$

where ΔH_f^0 is the heat of fusion of 100% crystalline PP and ΔH_f^* is the heat of fusion of the measured samples of PP or the graft copolymers.

The viscosity-average molecular weight of unmilled and milled PP was determined by viscometry according to the equation

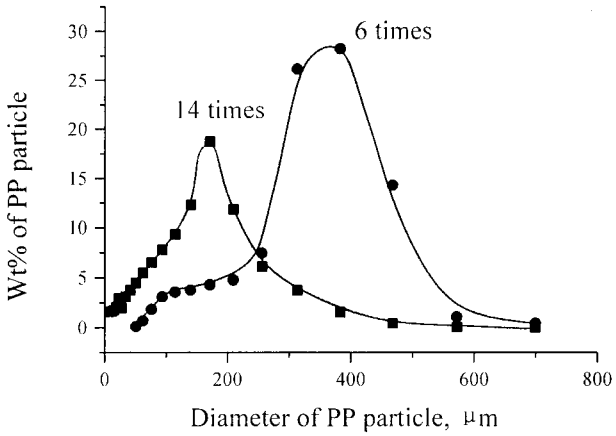

Figure 1 Particle-size distribution of milled PP; temperature: 18–40°C; rotation speed of pan mill: 30 rpm.

$$[\eta] = 1.9 \times 10^{-2} \overline{M}_{\eta}^{0.725}$$

(1,2,4-trichlorobenzene, 135°C) (3)

The melt-flow index of the PP and grafted PP were measured on a CS-127 melt-flow instrument at 230°C, with a load of 2.16 kg.

Samples for mechanical testing were prepared by injection molding. At least five specimens were tested in each case, and the deviation of the data around mean values was less than 5%. Tensile tests were done on an Instron universal testing machine 4302 at room temperature at a cross-head speed of 100 mm/min. Izod-notched impact strength tests were carried out with an XJ-40A impact tester.

RESULTS AND DISCUSSION

Pulverization and Degradation of PP During Pan Milling

Size Reduction of PP Particles During Pan Milling

The average size and size distribution of milled PP particles were studied using a particle-size measurement instrument (Fig. 1). The result shows that with increase of the number of milling cycles the average size of PP particles decreases quickly. The original particle size of PP had a 3–4-mm diameter. After 6 and 14 times of pan milling, the average particle size of PP decreases to 0.3- and 0.12-mm diameters, respectively. With increase of the number of milling cycles, the size-distribution curve of the PP particles moves to the zone of a smaller diameter, indicating that the pan-type milling equipment has a very high efficiency in pulverizing the brittle polymer PP.

Pulverization Dynamics of PP Particles During Pan Milling

Figure 2(a) shows that the percentage weight of milled PP particles with a diameter larger than r

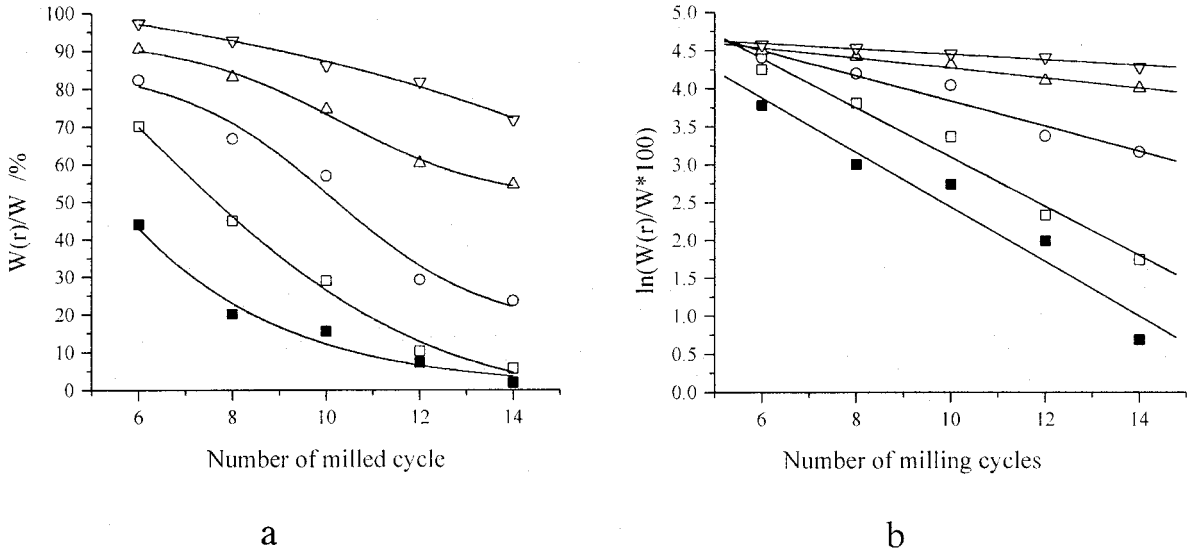

Figure 2 Relation between (a) $W(r)/W \times 100$ or (b) $\ln[W(r)/W \times 100]$ of PP particles and number of milling cycles: (■) r = 313 μm; (□) r = 256 μm; (○) r = 171 μm; (△) r = 114 μm; (▽) r = 76 μm.

μm [$W(r)/W \times 100$] decreases very fast from the sixth to the twelfth milling cycle and levels off later, a phenomenon similar to the relation between chemical reaction velocity and reactant concentration. Therefore, the pulverizing velocity of PP during pan milling may be analogized by drawing on the well-established chemical reaction velocity equation as below:

$$V = -dR/dN = kR \tag{4}$$

where V is the pulverizing velocity; R, the weight percent of PP particles larger than r μm after N milling cycles, $W(r)/W \times 100$; N, the number of milling cycles; and k, a constant. By integrating, we got

$$\ln R = -kN + \ln R_0 \tag{5}$$

where R_0 is the R value of unmilled PP.

Based on the size-distribution data of milled PP particles, we can obtain Figure 2(b) by plotting ln R, that is, ln[$W(r)/W \times 100$], versus N. The quite good linear relationship between ln R and the number of milling cycles verifies the dynamics equation proposed above. It is obvious that ln R decreases with increase of the number of milling cycles, and the slope ($-k$) of the lines increases with increase of the PP particle size, that is, the larger the PP particles, the faster the pulverizing velocity of PP during pan milling.

Degradation of PP During Pan Milling

Viscosity-average molecular weights of unmilled and milled PP were determined by viscometry. The viscosity-average molecular weights of PP unmilled and PP milled for 2, 4, 6, 8, 10, 12, and 14 times are 25.1×10^4, 22.8×10^4, 23.3×10^4, 22.6×10^4, 20.5×10^4, 21.4×10^4, 20.2×10^4, and 19.6×10^4, respectively. It is evident that the viscosity-average molecular weight of PP decreases with increase of the number of milling cycles, because the chain scission of PP takes place when it suffers from the quite strong pressure and shear forces. Figure 3 shows that the melt-flow index of milled PP also increases with increase of the number of milling cycles.

Effect of Pan Milling on the Structure of PP

DSC analysis (Table I) shows that the crystallinity of milled PP is less than that of PP, but its melting point and crystallization heat change little.

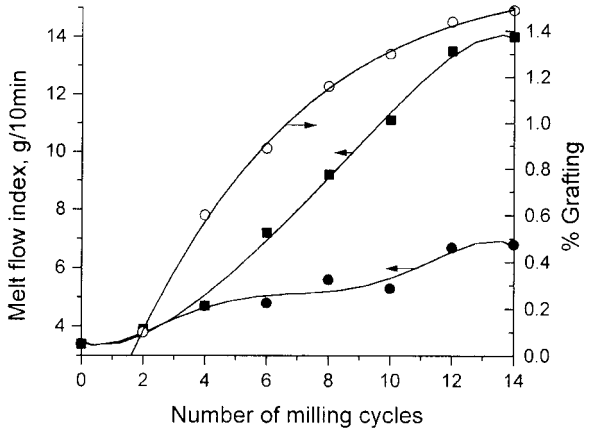

Figure 3 Effect of number of milling cycles and percentage of grafting of HMA onto PP on melt-flow indexes of PP-*g*-HMA and effect of number of milling cycles on melt-flow indexes of PP: (○,●) PP-*g*-HMA; (■) PP.

Solid-phase Grafting of HMA onto PP

When PP particles and HMA are pan-milled together, the macromolecular radicals generated from the chain scission of PP under stress can initiate HMA to polymerize, forming the PP-*g*-HMA graft copolymer. The graft copolymer PP-*g*-HMA was separated by water extraction to remove the unreacted monomer. The percentage of grafting was determined by chemical titration.

Effect of Experimental Condition on Graft Polymerization of HMA onto PP During Pan Milling

The effect of HMA content in the milled mixtures on the percentage of grafting and conversion of HMA is illustrated in Figure 4. With increase of the HMA content, the percentage of grafting increases, while the conversion decreases. When the HMA content is 1%, the percentage of grafting and conversion reach 0.41 and 41.41%, respectively. When the HMA content is 20%, the percentage of grafting reaches 2.07%, but the conversion decreases to 10.35%. The increase in the percentage of grafting for higher HMA content may be attributed to increase of the number of HMA molecules diffusing and reaching the free radical sites on the PP backbone during pan milling.

Table I Melting Point, Heat of Fusion, Crystallinity, Crystallization Temperature, and Heat of Crystallization of PP and PP-*g*-HMA

Polymer	T_m (°C)	ΔH_1 (J/g)	Crystallinity (%)	T_c (°C)	ΔH_2^* (J/g)
PP[a]	165.41	71.79	34.35	110.72	−94.85
PP[b]	165.60	65.38	31.28	125.75	−94.37
PP-*g*-HMA (Gr % = 1.49)[c]	166.06	64.42	30.82	129.10	−90.70
PP-*g*-HMA (Gr % = 1.49)[d]	165.41	68.21	32.64	127.62	−91.57

ΔH_1^* is heat of fusion; ΔH_2^*, heat of crystallization; and T_c, crystallization temperature.
[a] Extruded.
[b] Milled.
[c] Milled.
[d] Injected.

Figure 5 shows the effect of the number of milling cycles on the percentage of grafting of HMA onto PP and the BET surface area of PP-*g*-HMA. Both the percentage of grafting and the BET surface area increase with increase of the number of milling cycles. Further analysis revealed that there is a linear relation between the percentage of grafting and the BET surface area—an interesting phenomenon. Because pan milling results in both pulverization of PP particles and rupture of PP chains at the same time, the former leads to increase of the BET surface area of PP and the later generates macromolecular radicals to initiate graft polymerization of HMA onto PP.

Figure 6 shows that the effect of temperature on the percentage of grafting of HMA onto PP is quite complicated. In our experimental range, increasing temperature promotes diffusion of the HMA molecules, favoring increase of the percentage of grafting of HMA onto PP, but hampers the mechanochemical degradation of PP, that is, the rupture of PP chains and generation of macromolecular radicals, resulting in decrease of the percentage of grafting of HMA onto PP. As a result, when the temperature of PP before milling is low and the temperature during pan milling is high, the percentage of grafting of HMA onto PP is the highest.

The effect of rotation speed of the pan mill on the percentage of grafting is shown in Figure 7. In our experimental range, the percentage of grafting of HMA onto PP increases with increase of the rotation speed of the pan mill, because with increase of the rotation speed of the pan mill, the shear forces increase and the number of macromolecular radicals generated through chain scission of PP increases. The low percentage of graft-

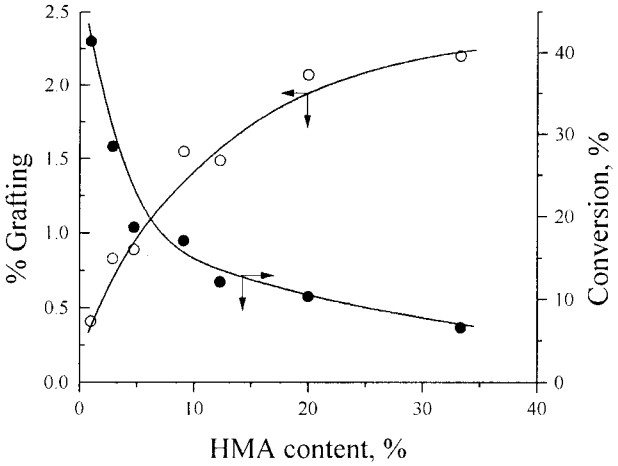

Figure 4 Effect of HMA content in the milled mixture on percentage of grafting and conversion of HMA; rotation speed: 30 rpm; temperature: 18–40°C.

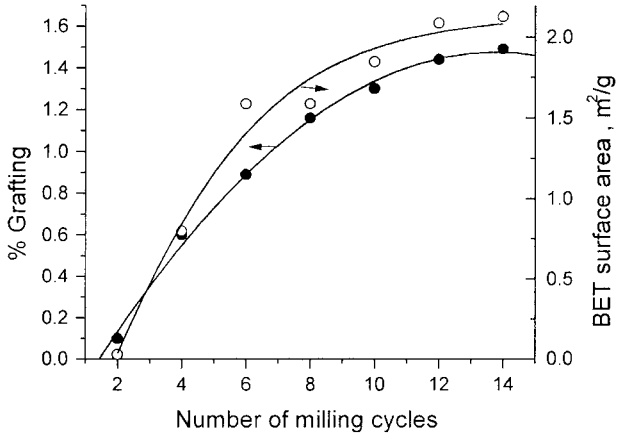

Figure 5 Effect of number of milling cycles on percentage of grafting of HMA onto PP and BET surface area of PP-*g*-HMA; rotation speed: 30 rpm; temperature: 20–50 °C.

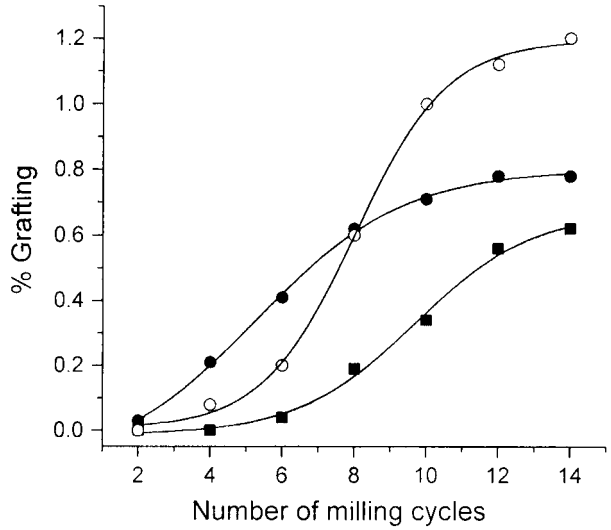

Figure 6 Effect of temperature on solid graft polymerization of HMA onto PP: HMA/PP (wt %): 5%; rotation speed: 30 rpm; temperature: (■) 18°C before milling, 18–35°C during milling; (●) 18°C before milling, 35–50°C during milling; (○) 8°C before milling, 8–30°C during milling.

ing at a rotation speed of 40 rpm and the number of milling cycles of less than 8 may be attributed to the low temperature during pan milling. When the rotation speed is less than 20 rpm, or higher than 50 rpm, the milling of PP becomes difficult.

Characterization of the Graft Copolymer PP-g-HMA

The difference in the FTIR spectra of PP and grafted PP confirms the graft polymerization of HMA onto PP via pan milling, because the characteristic bands of secondary amido at 1664.27 and 1536.99 cm^{-1} appear in the FTIR spectrum of the graft copolymer, but are absent in the FTIR spectrum of PP.

Contact angle measurement shows that the contact angle of water on PP is 85°; the contact angle of water on PP-*g*-HMA films is smaller than that on PP and decreases with increase of the percentage of grafting of HMA. When the percentage of grafting of HMA on PP is 0.1 and 1.49%, the contact angles of water on the graft copolymers are 75°and 56°, respectively, indicating the polarity enhancement of graft copolymers owing to the grafting polymerization of the polar monomer HMA onto PP.

Table I lists the data obtained from DSC analysis. The exothermal peak appears at 110.72°C for PP and 127.62°C for PP-*g*-HMA, respectively, indicating a much higher crystallization temperature for the graft copolymer as compared with PP, due to the grafted HMA which acts as a nucleating agent. These results are consistent with the observation reported by Sathe for PP-*g*-MAH.[17] From Table I, it also can be seen that the heat of fusion of PP-*g*-HMA decreases as compared with PP due to incorporation of HMA into PP.

Table II shows that the tensile strength of PP-*g*-HMA is higher than that of PP, owing to stronger intermolecular interaction for PP-*g*-HMA of higher polarity. But the Izod notched impact strength of PP-*g*-HMA decreases as compared with PP, probably due to decrease in the molecular weight of PP-*g*-HMA. For PP-*g*-HMA, the improvement in mechanical properties is obvious by comparison with the milled PP samples.

From Figure 3, it can also be seen that (1) the melt-flow indexes of graft copolymers increase slowly with increase of the number of milling cycles and (2) the graft copolymers have lower melt-flow indexes than those for the milled PP when the number of milling cycles is the same. Because pan milling results in both a decrease of molecular weight for milled PP or PP-*g*-HMA and an increase of the percentage of grafting, the former leads to increase of the melt-flow index of PP-*g*-HMA, but, contrarily, the latter, to increase of the molecular interaction.

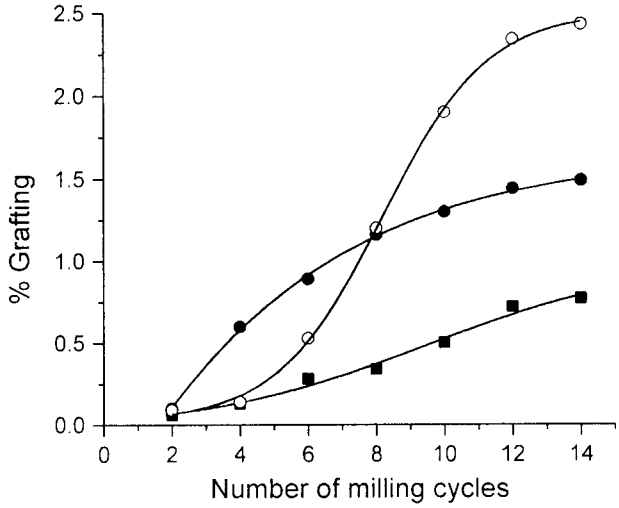

Figure 7 Effect of rotation speed of pan mill on solid graft polymerization of HMA onto PP: HMA/PP (wt %): 14%; (■) 20 rpm, 10–35°C; (●) 30 rpm, 20–50°C; (○) 40 rpm, 15–50°C.

Table II Mechanical Properties of PP, Milled PP, and PP-*g*-HMA

Polymer	No. Milling Cycles	Percentage of Grafting (%)	Tensile Strength (MPa)	Elongation at Break (%)	Izod Notched Impact Strength (J/m)
PP	0	—	34.94	32	19.4
PP	4	—	34.06	9	15.1
PP	8	—	34.96	11	—
PP-*g*-HMA	8	1.16	37.53	27	14.6
PP-*g*-HMA	14	1.49	38.38	23	16.5

CONCLUSIONS

The pan-type milling equipment has a unique structure and a high efficiency in a solid-phase polymer stress reaction. Suffering from the quite strong stress exerted by the pan mill, the particle-size reduction and chain scission of PP take place and the formed macromolecular free radicals can initiate further reactions.

The solid-phase grafting of HMA onto PP can be realized by comilling PP with HMA together using the novel pan-type milling equipment. The percentage of grafting of HMA onto PP reaches 0.41–2.43%, depending on HMA content, number of milling cycles, temperature, and rotation speed of the pan mill. Compared with other methods used for solid-phase grafting of PP, the technique reported here has advantages such as low reaction temperature, no initiator or solvent added, *in situ* compatibilizing during polymer processing, and easy commercialization.

The authors are grateful for the financial support from the China Petro-Chemical Science &Technology Development Corp. and the Polyamide Research Center of the China Petro-Chemical General Corp.

REFERENCES

1. Porter, R. S.; Casale, A. Polym Eng Sci 1985, 25, 129.
2. Barambom, N. K. Mechanochemistry of Polymer; Maclaren: London, 1964.
3. Simionescu, C.; Vasilin-oprea, C. Mechanochemia Compusilor Macromoleculari; Academic Republicii Socialiste: Bucharest, 1967 (in Romanian).
4. Bristow, G. M.; Watson, W. F. In The Chemistry and Physics of Rubber-like Substances; Baremam, L., Ed.; Wiley: New York, 1963; Chapter 14.
5. Casale, A.; Porter, R. S. Polymer Stress Reactions; Academic: New York, 1978; pp 1–7.
6. Shen, Y.; Chen, K.; Wang, Q.; Li, H.; Xu, X. J Macromol Sci A Chem 1986, 23, 1415.
7. Xu, X.; Wang, Q.; Li, H. J Macromol Sci A Chem 1986, 23, 1433.
8. Chen, K.; Xu, X. J Macromol Sci A Pure Appl Chem 1992, 29, 55.
9. Xu, X.; Wang, Q.; Kong, X. A. Plast Rubb Compos Process Appl 1996, 25, 152.
10. Wang, Q.; Cao, J. Z.; Huang, J. G.; Xu, X. Polym Eng Sci 1997, 37, 1091.
11. Xu, X.; Wang, Q. CN Patent CN2 217 463Y, 1995.
12. Wang, Q.; Liu, C. L. In 14th Meeting of Polymer Processing Society, Yokohama, Japan, June 8–12, 1998; p 633.
13. Ruggeri, G.; Aglietto, M.; Petragnani, A.; Ciardelli, F. Eur Polym J 1983, 19, 863.
14. Rengarajan, R.; Vicic, M.; Lee, S. J Appl Polym Sci 1990, 39, 1783.
15. Minoura, Y.; Ueda, M.; Mizunuma, S. J Appl Polym Sci 1994, 53, 1625.
16. Roover, B. D.; Sclavons, M.; Carlier, V. J Polym Sci Part A Polym Chem 1995, 33, 829.
17. Sathe, S. N.; Rao, G. S. S.; Devi, S. J Appl Polym Sci 1994, 53, 239.
18. Cheng, D. W. Chin Chem World 1991, 7, 322.